DOI: 10.31265/atnrs.774

Hydrophobic Modification of Bentonite: Unravelling the Impacts of Aluminium Cation on Silica-Water Interface

Hazzaz Bin Yousuf[1]*, Seyed Hasan Hajiabadi[1], Pouya Khalili[1], Mahmoud Khalifeh[1]

[1]Department of Energy and Petroleum Engineering, Faculty of Science and Technology, University of Stavanger, 4036 Stavanger, Norway

ABSTRACT

Silica, a predominant metal oxide and fundamental component of the Earth's crust, exerts significant influence on diverse geochemical and industrial processes through its interactions with water. This study delves into the surface modification of bentonite clay, as a naturally occurring aluminosilicate source, via treatment with varied concentrations of $Al(NO_3)_3$, as a novel surface modification approach, and H_2SO_4, as a control technique. The obtained results elucidated important alterations in micro-scale surface characteristics, colloidal stability, and rheological behaviour of the aqueous solutions derived from the modified bentonite samples. Zeta potential analyses showed shifts from a stable colloidal solution in untreated bentonite to heightened instability following aluminium nitrate (and acid) treatment(s). In addition, micro-scale surface analyses employing scanning electron microscope (SEM) with energy dispersive spectroscopy (EDS) and Fourier-transform infrared (FTIR) revealed significant changes, encompassing heightened degree of coagulation, caused by intensified neutralization, and diminished swelling capacities induced by surface modifications. EDS analysis validated cation exchange processes and intensified agglomeration with $Al(NO_3)_3$ treatment. Furthermore, the stability and rheological behaviour of resulting aqueous fluids demonstrated reduced stability in $Al(NO_3)$-treated samples, comparable to acid-treated samples, indicative of hydrophobic surfaces post-treatment. The findings highlighted the effectiveness of the applied treatment technique, emphasizing practical implications for surface-treated bentonite utilization in different environments. However, observed variations influenced by ion type and concentration prompt the imperative for further research to unveil specific mechanisms of treatment approaches on aluminosilicate systems. This endeavour contributes to advancing comprehension and optimization of silicate performance across diverse applications.

Keywords: Bentonite, Surface Modification, Cation Exchange and Adsorption, Hydrophobicity.

*Corresponding authors: Hazzaz Bin Yousuf (Email: Hazzaz.b.yousuf@uis.no)

INTRODUCTION

Surface science and interfacial chemistry play a pivotal role in unravelling the intricate structures of material surfaces and their interactions with the surrounding environment[1, 2]. While extensive research has focused on water behaviour at metal oxide interfaces, the hydrophilicity/hydrophobicity attributes of silicate/aluminosilicate surfaces, particularly due to the prevalence of silica within solid oxides, have become a subject of significant investigation [3-7]. Despite the numerous studies conducted on the hydrophilic aspects of these components, the distinct hydrophobic surface properties remain a critical aspect with far-reaching implications. The hydrophobic properties of these surfaces, driven by the reactivity of silanol groups enabling chemical modifications, have found applications in advanced catalysis, biomedical/biosensing technologies, composite materials, pharmaceuticals, cosmetics, civil engineering, and environmental applications[5, 8-10].

An emerging field of aluminosilicate applications involves the use of hydrophobic aluminosilicates in geopolymer (GP) systems, presenting an environmentally friendly alternative to Ordinary Portland Cement (OPC) with significantly lower greenhouse gas emissions during production[11-13]. Silica surface modification has proven effective in addressing challenges associated with large-scale GP applications, such as efflorescence and carbonation uncertainties[14-17]. Surface transformation towards hydrophobicity plays a crucial role in suppressing capillary absorption, water diffusion, alkali ion leaching, and efflorescence/carbonation, while mitigating shrinkage in GPs.

The surface chemistry of aluminosilicates also plays a pivotal role in altering the characteristics of drilling fluids, particularly in oil-based drilling fluids[18]. Surface modification of bentonite, an inherently hydrophilic aluminosilicate clay, significantly impacts the stability of oil-based drilling fluids. Organoclays, formed by such modifications, serve as additives that enhance filtration characteristics, provide favourable dispersing properties in the oil phase, and contribute to essential rheological characteristics for drilling wells[2, 19-21].

Various methodologies contribute to increased hydrophobicity of aluminosilicate surfaces, especially in clay minerals such as bentonite[2, 22-26]. Acid treatment, as one of the most prominent techniques, enhances adsorption efficiency and catalytic properties by replacing interlayer exchangeable cations (Na^+, K^+, Ca^{2+}) with H^+ ions, causing dissolution of aluminium octahedral and silicon tetrahedral sheets[18, 27-32]. However, challenges in monitoring structural modifications during acid treatment pose concerns in drilling fluid and catalysis applications[31]. In addressing these challenges, one widely accepted approach for surface modification of bentonite samples involves neutralizing bentonite platelet charges through the adsorption of chemical agents, such as surfactants, cationic polymers, or even certain metal cations[22, 24, 33, 34]. Notably, Al^{3+} ions exhibit high adsorption capacity towards bentonite surfaces, as evidenced by numerous studies, particularly in wastewater management applications[35-38]. Despite promising results regarding the high capacity of bentonite for Al^{3+} adsorption, a notable gap exists in the literature concerning the impacts of these interactions on the hydrophobic characteristics of clay particles.

This study aims to address these gaps by applying two distinct surface modification techniques to bentonite (selected as the aluminosilicate source), including the application of aluminium nitrate, and acid treatment, as a control modification technique. The primary objectives are to demonstrate the influential parameters shaping the surface chemistry of

bentonite after employing the treatment approaches and to explore the potential of Al^{3+} ions in surface modification of aluminosilicate species. A combination of characterization techniques, including Zeta-potential measurement, Fourier-transform infrared (FTIR) analysis, and scanning electronic microscopy (SEM) equipped with a backscattered electron detector (BSD) and an energy dispersive spectroscopy (EDS) analysis, was employed to evaluate chemical/structural alterations induced by the surface modification treatments. Then, the efficacy of the novel hydrophobic technique ($Al(NO_3)$) was assessed through analyzing the stability and rheological behavior of the aqueous solutions prepared by implementing the surface-modified bentonites.

METHODS

Figure 1 illustrates the experimental methodology employed in this study.

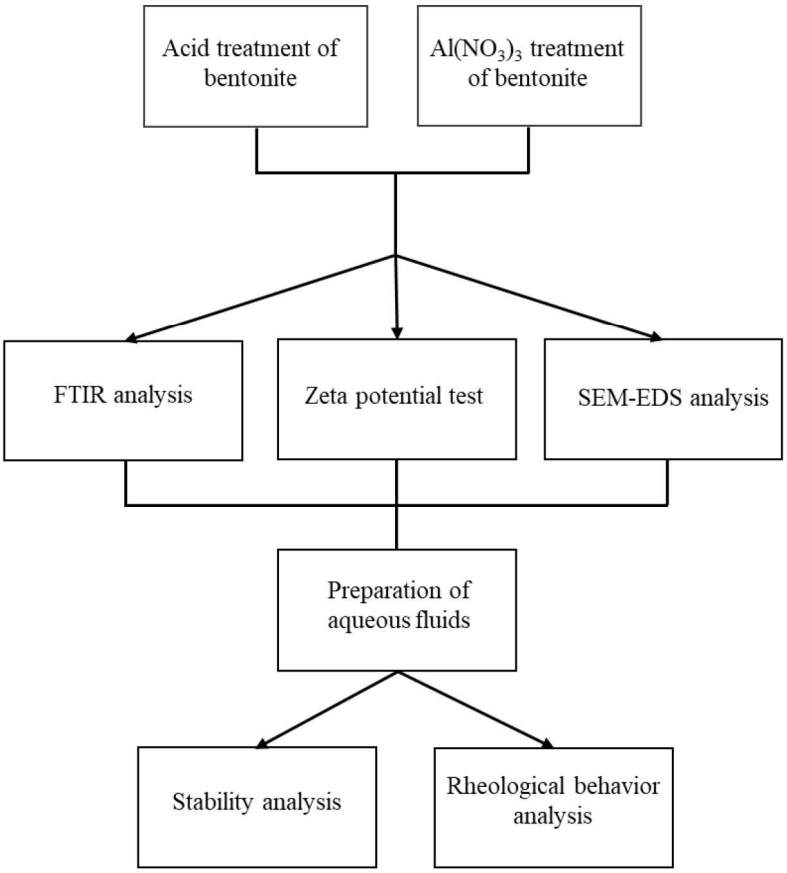

FIGURE 1: A flowchart showing the experimental steps of this study.

Materials

Natural bentonite was obtained from the Schlumberger Norge AS, Norway. Concentrated sulfuric acid, with a purity range of 95-97%, was purchased from Merck. Aluminium nitrate nonahydrate was procured from Sigma-Aldrich.

Surface modification approaches

Acid treatment

Adhering to the procedures outlined by Tyagi et al.[31] and Tomić et al.[39], the raw bentonite underwent purification through sedimentation to eliminate impurities prior to usage. Specifically, 10 grams of the bentonite were vigorously stirred in 1 L of distilled water and left to sediment for 24 hours. The upper 2/3rd fraction of the supernatant was separated, dried in oven under 40 °C for two nights, then finely powdered and sieved to achieve a particle size of 150 mesh. Subsequently, 1 gram of the purified bentonite was refluxed with H_2SO_4 (5 mL) at two concentrations (5N, and 10N) at 80 °C for 4 hours. After cooling, the resulting slurry was filtered, and the solid residue was thoroughly washed with hot distilled water until achieving a pH of 7. The washed product was initially dried at room temperature, followed by a 6-hour drying period at 120 °C. The resulting bentonite was then finely powdered and sieved to a particle size of 150 mesh. The acid-treated bentonite clays, denoted as 5N and 10N, were subsequently employed in the formulation of aqueous fluids designated as F-1 and F-2, respectively.

Aluminium nitrate treatment

As previously mentioned, owing to the demonstrated heigh adsorption capacity of Al^{3+} ions onto clay minerals, this study investigates the potential impact of aluminium nitrate ($Al(NO_3)_3$) on the hydrophobic characteristics of silica surfaces. For this purpose, three distinct aqueous fluid formulations, designated F-3, F-4, and F-5, were formulated by incorporating 0.05, 0.1, and 0.15 wt.% $Al(NO_3)_3$, respectively, into the initial base fluid system.

Based on the existing literature, the interactions between bentonite and aluminium nitrate result in notable increases in the basal spacing of bentonite. This shift indicates the adsorption of Al^{3+} ions into the interlayer spaces. The interlayer adsorption mechanism involves electronic attraction (Eq. (1)) and interlayer cation exchange reactions of Al^{3+} ions with interstratified Na^+ ions (Eq. (2)).

$$\equiv X^- + Al^{3+} \rightleftharpoons \equiv X_3^-.Al^{3+} \quad (1)$$

$$3 \equiv X^-.Na^+ + Al^{3+} \rightleftharpoons \equiv X_3^-.Al^{3+} + 3Na^+ \quad (2)$$

Surface complexation, and precipitation are other mechanisms contributing to the interaction between Al^{3+} and bentonite[40, 41].

Characterization

The examination of the chemical bonds within surface-modified bentonites involved FTIR analysis using an Agilent Cary 630 (the United States). The FTIR experiments, conducted over a wavelength spectrum ranging from 650 to 4000 cm^{-1}, elucidated the chemical bonds of the bentonites by assessing the absorption of infrared light at different frequencies. Concurrently, the evolving microstructures of the bentonites were scrutinized through a Zeiss Supra 35VP model scanning electron microscope (SEM) equipped with a backscattered electron detector (BSD) and an energy dispersive spectroscopy (EDS) analyser.

In preparation for these analyses, the samples underwent drying at 40°C overnight and subsequent storage in a vacuum dryer for one day to eliminate residual moisture. Powdered samples were employed for both FTIR and SEM-EDS analyses.

Preparation of aqueous fluids

Aqueous solution of local bentonite was formulated as the "Base fluid" by adding 15.24 gr of the untreated bentonite to 100 mL of deionized water, resulting in a density of 1.089 gr/cm^3. Concurrently, analogous aqueous fluids, denoted as F-1 and F-2, were systematically produced through the introduction of bentonites treated with 5N and 10N H_2SO_4 to an equivalent volume of deionized water, respectively. In addition, F-3, F-4, and F-5 were prepared by the incremental addition of aluminium nitrate ($Al(NO_3)_3$) at concentrations of 0.05 wt.%, 0.1 wt.%, and 0.15 wt.% to the Base fluid. Table 1 lists the array of fluids designed for the purposes of this investigation.

TABLE 1: A list of fluids employed in this research.

Aqueous fluid	Treating approach	Normality/concentration of treating agent
Base fluid	-	-
F-1	H_2SO_4	5N
F-2	H_2SO_4	10N
F-3	$Al(NO_3)_3$	0.05 wt.%
F-4	$Al(NO_3)_3$	0.1 wt.%
F-5	$Al(NO_3)_3$	0.15 wt.%

Flow behaviour and stability analyses

The rheological analyses were conducted using a rotational rheometer (MCR 302e, Anton Paar, Austria) operating under ambient temperature conditions. Shear stress measurements were taken from 0.1 to 500 1/s in ascending order with 10 second duration between each measurement point, followed by descending order from 500 to 0.1 1/s. The average stress measurement was used to plot the flow curve and obtain flow parameters. Thus, information about the thixotropy could not be obtained from the flow curve. To conduct rheological analyses, 80 mL of each fluid were prepared. The rheological characteristics of the fluids were described using the Bingham plastic model, which is widely known as the primary rheological model for bentonite-based fluids:

$$\tau = \tau_0 + \mu_p \dot{\gamma} \tag{3}$$

Here, τ is the shear stress, τ_0 represents the yield stress, $\mu_p$is the plastic viscosity, and $\dot{\gamma}$ denotes the shear rate.

The assessment of fluid stability involved a free-fluid test with a stationary phase conducted at room temperature. This procedure utilized a graduated cylinder markings at 1 mL intervals. Following the introduction of fluids into the graduated glass cylinder, filling it to the 20 mL

level, distinct undisturbed intervals were meticulously observed to quantify the height of the free fluid at the top of the fluid solution.

RESULTS AND DISCUSSION

This section provides the results of characterization methods, rheological analyses, and stability tests, employed to analyse the impact of treating approaches on the surface chemistry of the bentonite samples.

Characterization of surface-modified bentonite clays
Zeta potential analysis

Table 2 represents the results of Zeta potential analysis quantifying the surface characteristics of untreated and treated bentonite samples with different concentrations of acid and $Al(NO_3)_3$. In its untreated state, the bentonite solution displayed a Zeta potential of -32.07 mV, indicative of a stable colloidal solution. However, the bentonite samples treated with 5N H_2SO_4 and 10N H_2SO_4 treatments showed Zeta potential values of -17.07 mV and -16.52 mV, respectively, suggesting a shift towards higher degree of instability. Likewise, the modification of bentonite surfaces with $Al(NO_3)_3$ at different concentrations resulted in higher Zeta potential values compared to the untreated bentonite sample (-21.56 mV, -18.94 mV, and -14.62 mV at 0.05, 0.1, and 0.15 wt.% of $Al(NO_3)_3$, respectively).

Overall, these findings revealed the pronounced affinity of untreated bentonite (specifically smectite or montmorillonite particles) to adsorb cations, as a compensatory mechanism for the elevated negative charge. However, the obtained results signified that despite the surface modification treatments, the clay particles maintained a net negative charge. This observation is due to the equilibrium established between the permanent surface charges, initially caused by the isomorphic substitution of lower valency metal ions within the clay structure, and the edge charges. Throughout surface modification treatments, although a degree of adsorption and cation exchange occurs in the basal faces responsible for the permanent charges, the introduced cations (H^+ or Al^{3+}) predominantly adsorb to (or undergo cation exchange with) the edge charges. However, this process does not adequately counterbalance the net negative charges of the bentonite samples due to the relatively limited edge surface area, potentially constituting as little as 5-10% of the total surface area. This is notably lower than the permanent negative charges concentrated on the basal face, which predominantly contributes to the overall surface charge density of the bentonite[40-42].

TABLE 2: The results of Zeta potential analyses of untreated and treated bentonite samples.

Normality/concentration of treating agent	Zeta potential (mV)
Bentonite	-32.07
5N H_2SO_4	-17.07
10N H_2SO_4	-16.52
0.05 wt.% $Al(NO_3)_3$	-21.56
0.1 wt.% $Al(NO_3)_3$	-18.94
15 wt.% $Al(NO_3)_3$	-14.62

FTIR analysis

Figure 2 illustrates the Fourier-transform infrared (FTIR) spectra of diverse bentonite samples, encompassing untreated specimens and those treated with H_2SO_4 and $Al(NO_3)_3$. These spectra describe distinct vibrational modes corresponding to the molecular structure of bentonite. The spectral region of 3700–3200 cm^{-1} reveals vibrations associated with water molecules in the interlayers and structural hydroxyl groups within the bentonite clay layers. The range of 1300–650 cm^{-1} is where primary silicate bands will[43, 44].

Prior to activation, the spectrum reveals prominent O-H stretching vibrations of O-H groups coordinated to octahedral Al^{3+} cations at 3620 cm^{-1} wavenumber [43, 44]. A noteworthy peak at 3403 cm^{-1} indicates O-H asymmetric stretching from Al–OH, Si–OH, and H-O-H vibrations of adsorbed water molecules[33, 34]. Additionally, the angular deformation of the H–O–H bond in interlayer water molecules is evident at 1636 cm^{-1} wavenumber [33]. Peaks from external clay components, such as quartz and dolomite, appear at 790 and 698 cm^{-1}, respectively, while the peak at 1112 cm^{-1} represents the longitudinal Si–O stretching mode [33, 43, 44]. Additionally, T-O-T (T=Si, Al) stretching peaks associated with the tetrahedral layer are distinctly visible at 988 cm^{-1}, and OH bending peaks related to the octahedral layer are observed at 913 and 876 cm^{-1} (caused by Al–Al–OH or Al–Fe–OH vibrations) [31, 43, 44]. Importantly, the band at 1142 cm^{-1} signifies the stretching vibrations of O-C-O bonds, indicating the adsorption characteristics of carbonate groups[13].

Upon acid activation, as the control surface modification technique, protons (H^+) derived from H_2SO_4 permeated the layers of bentonite, binding to hydroxyl (OH) groups. This led to dihydroxylation and partial dissolution of the smectite structure. Observable alterations in the characteristic absorption bands in the FTIR spectra post-acid attack include a slight deviation in the positions of O-H stretching bands and reduced intensities of O-H stretching bands at 3620 cm^{-1}. The disappearance of the band at 3403 cm^{-1} resulted from the partial dissolution of the primary bentonite structure. Wavenumber shifts and significant intensity decreases in the band at 1621 cm^{-1}, associated with adsorbed water (H–O–H stretching vibrations), were noted in comparison to the untreated bentonite at 1636 cm^{-1}, attributed to the loss of adsorbed water resulting from the relatively high temperature generated during the activation process. The sharp vibration band near 1112 cm^{-1}, identified as the stretching vibration of the Si–O group, exhibited a slight shift to higher wavenumbers and lower intensity after the acid attack. These

observations are indicative of dissolution during acid activation[34]. In summary, minor shifts and intensity decrease in certain bands highlighted the significant impact of acid treatment on H^+ ion interaction[13, 34]. This interaction likely involves surface functional groups, leading to the formation of a hydrophobic, partly protonated silica phase as the end product[34, 43, 44].

$Al(NO_3)_3$ treatment of bentonite induces discernible alterations in the FTIR spectra. The intensified peak at 3403 cm^{-1} denotes an elevated O-H asymmetric stretching, indicative of successful integration of Al–OH functionalities onto the bentonite surface. The increased intensity around 986 cm^{-1} suggests the presence of Al-O-Al bonds, highlighting alterations in the aluminium coordination environment, potentially arising from interactions with the bentonite matrix. The intensified peak at 1636 cm^{-1} implies the changes in water interactions within the interlayer spaces [45]. Notably, the emergence of a weak band at 840 cm^{-1} signifies the formation of new Al-OH bonds, possibly in the form of Al–OH–Mg bonds, highlighting the introduction of novel chemical functionalities through $Al(NO_3)_3$ modification[31,45, 46]. Additionally, sharp peaks at 1349 cm^{-1} are associated with the stretching vibration of nitrate ions (NO_3^-), confirming the successful incorporation of nitrate ions onto the bentonite surface[45].

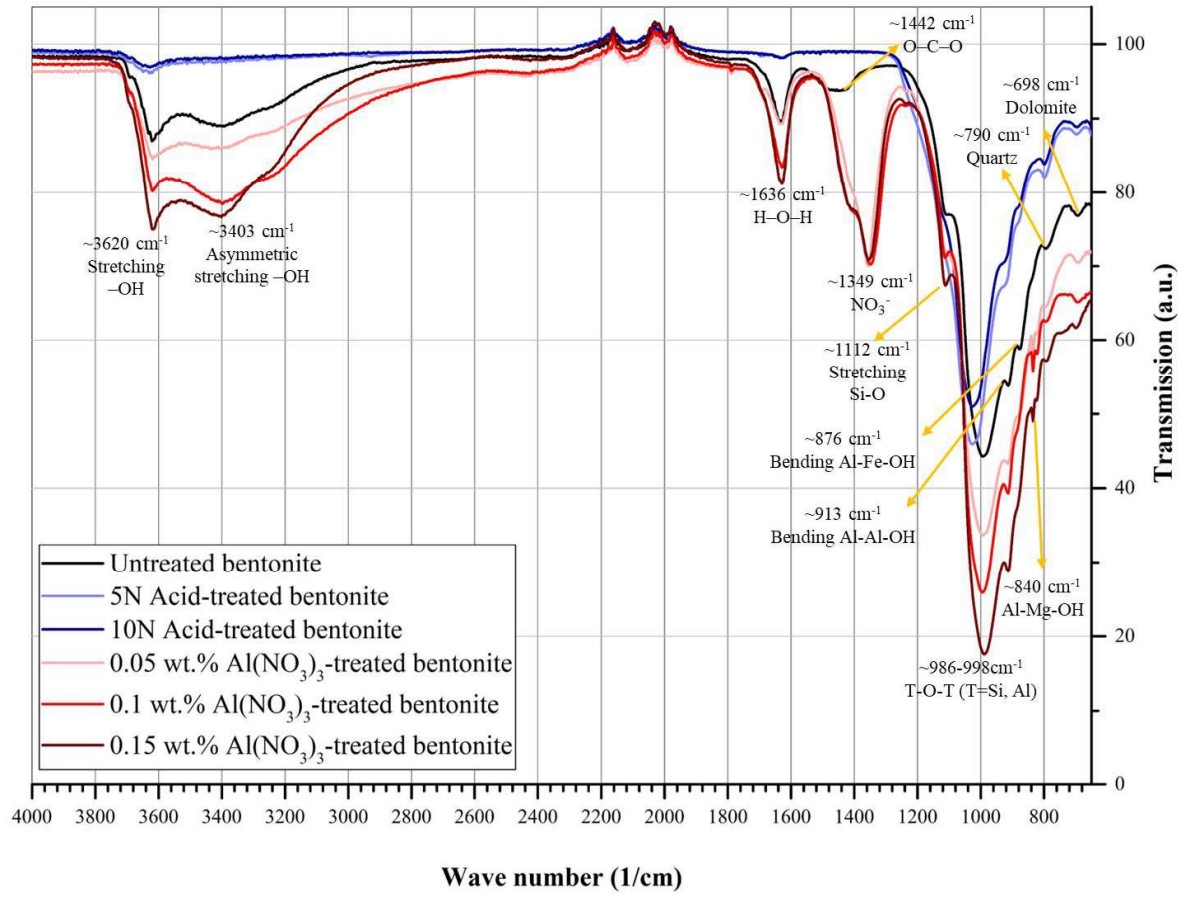

FIGURE 2: Fourier Transform Infrared Spectroscopy (FTIR) spectrum of untreated (raw) and treated (with varying concentrations of H_2SO_4 and $Al(NO_3)_3$) bentonite samples.

SEM-EDS analysis

The dried powder samples of the bentonites (untreated and treated) were studies using an SEM-BSD with EDS analysis. Selected micrographs are presented in Figures 3 to 8. SEM-BSD/EDS analysis of the untreated bentonite sample (Figure 3) reveals the homogenous surface, with layered structure (platelet shapes) and flacked morphology of the bentonite sample. This layered arrangement, featuring alternating layers of aluminium octahedral sheets and silica tetrahedral sheets, contributes to the hydrophilic properties of bentonite and its ability to swell and absorb water[47] . In addition, platelets morphologies with a ridged, crinkly, and honeycomb-like texture can be characteristic of the smectites groups[47].

The micrographs of the bentonite samples treated with 5N (Figures 4) reveal a constrained sheet-like structure of the bentonite following treatment with H_2SO_4. This alteration in structure is due to the modification of surface charge properties induced by cation exchange, which involves the substitution of exchangeable cations on the bentonite with protons, thereby diminishing the electrostatic repulsion between colloidal particles. The heightened acidity (10N H_2SO_4) has even caused more substantial structural transformations in the bentonite samples, resulting in the disintegration of the clay structure. These alterations lead to an augmented hydrophobicity of the bentonite, enhanced particle coagulation, reduced swelling capacity, ultimately contributing to diminished stability of the fluid, as illustrated in Figure 5.

Furthermore, the bentonite samples subjected to treatment with 0.05 wt.% $Al(NO_3)_3$ (Figure 6) showed a more compact layer of smectites characterized by rigid, irregular structures. Notably, heightened degrees of agglomeration were observed in bentonite samples treated with 0.1 wt.% and 0.15 wt.% $Al(NO_3)_3$, indicating an intensified neutralization of bentonite surface charges, potentially attributed to an elevated level of cation exchange (Figures 7 and 8). These observations are consistent with Zeta-potential analysis findings, wherein the specimen treated with 0.15 wt.% $Al(NO_3)_3$ exhibited the most significant shift towards achieving a neutralized surface charge. Consequently, this neutralization enhances hydrophobic forces, resulting in an increased rate of particle agglomeration and flocculation.

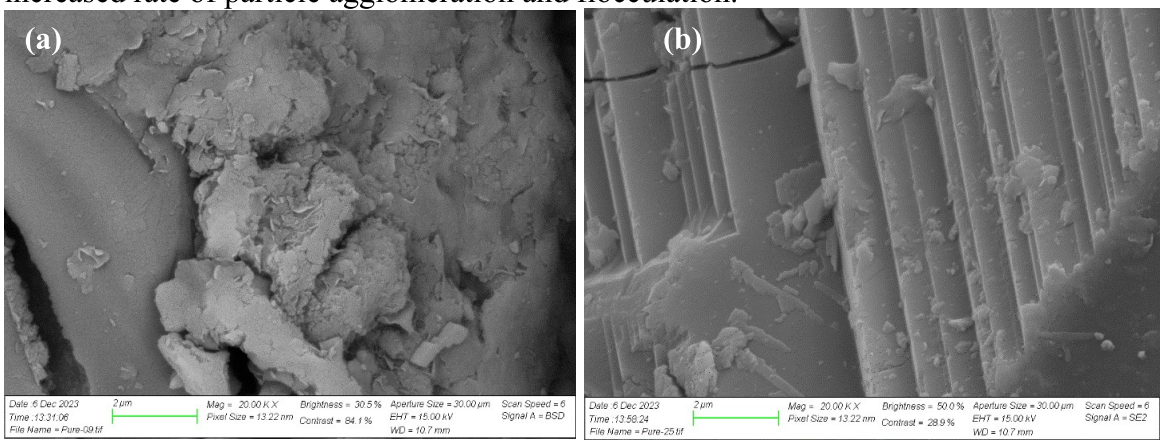

FIGURE 3: SEM-BSD images of untreated bentonite samples.

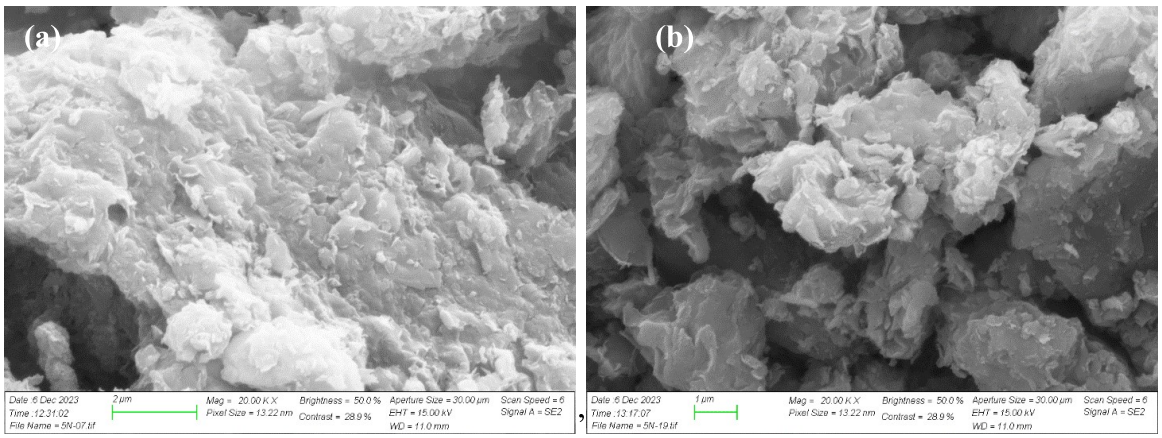

FIGURE 4: SEM-BSD images of 5N acid-treated betonite samples.

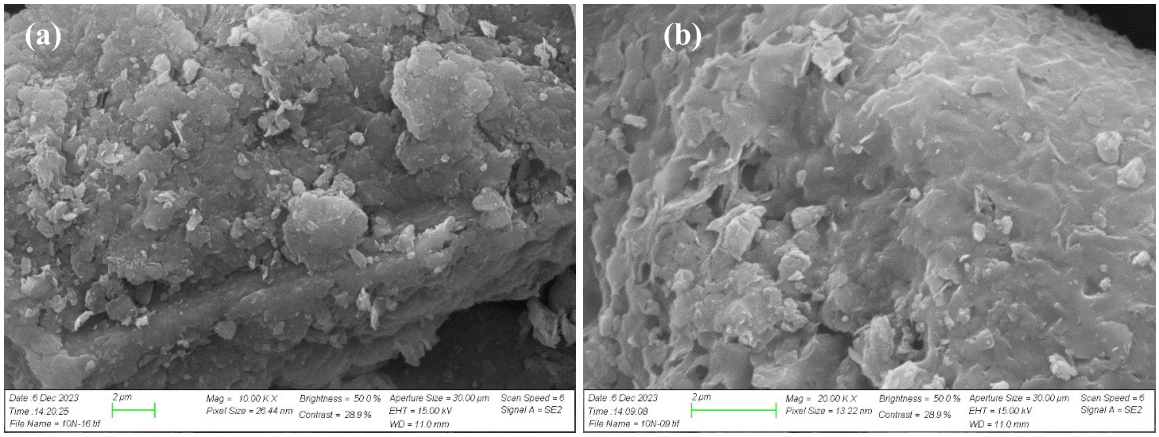

FIGURE 5: SEM-BSD images of 10N acid-treated bentonite samples.

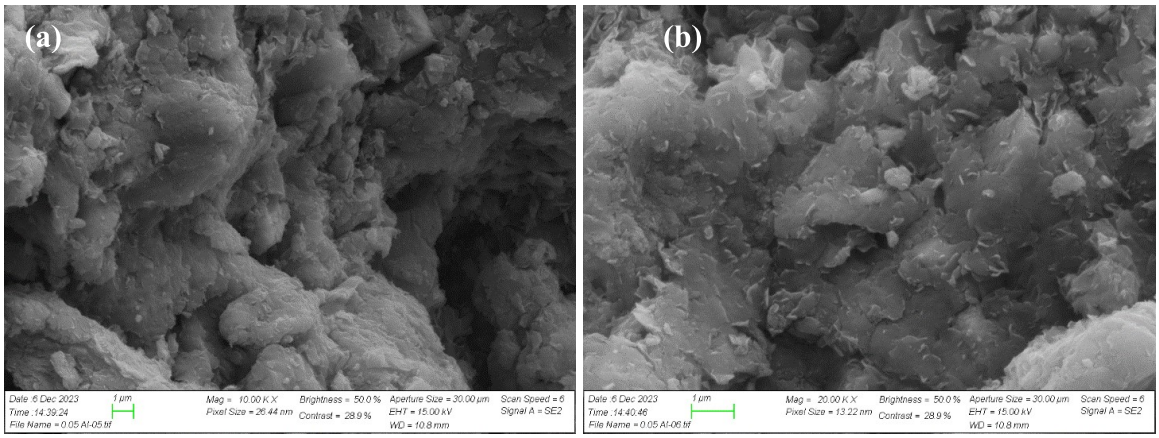

FIGURE 6: SEM-BSD images of 0.05 wt.% $Al(NO_3)_3$-treated bentonite samples.

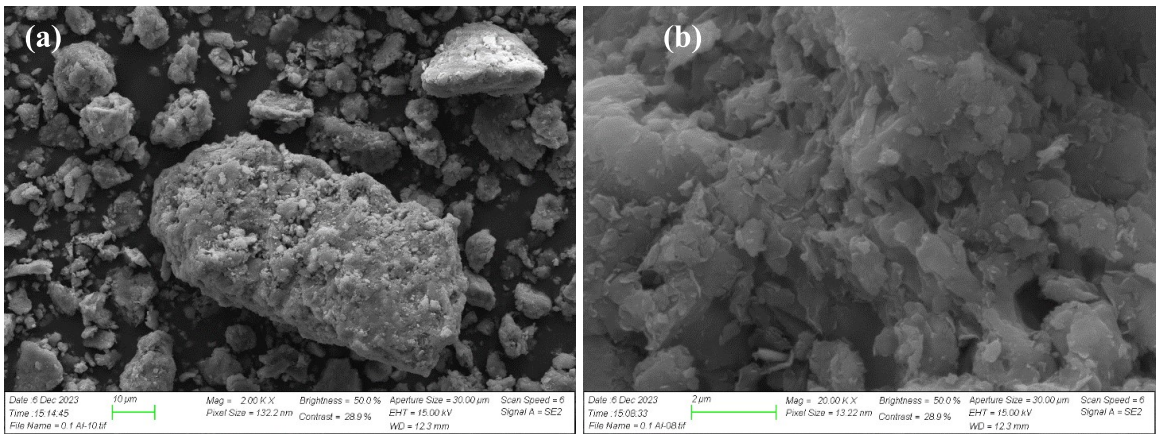

FIGURE 7: SEM-BSD images of 0.1 wt.% $Al(NO_3)_3$-treated bentonite samples.

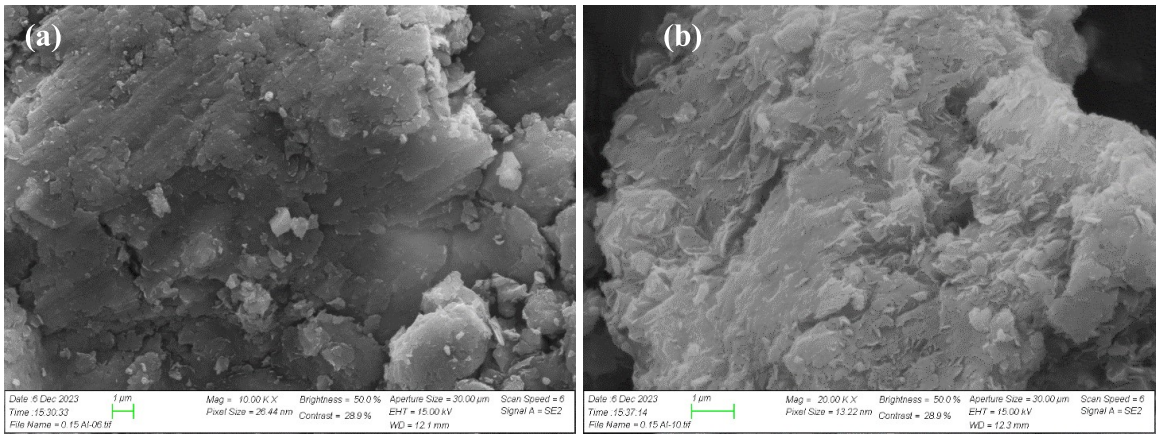

FIGURE 8: SEM-BSD images of 0.15 wt.% $Al(NO_3)_3$-treated bentonite samples.

The mean cationic composition within each bentonite sample, derived from different areas of the sample surface, is illustrated in Figure 9. Evidently, the application of modification methodologies to the bentonite surface has led to diminished concentrations of monovalent ions (Na^+ and K^+) on the clay surface. This can be ascribed to cationic exchanges induced by H^+ or Al^{3+} ions. This observation is also in accordance with the heightened Al content on the surface of bentonite samples treated with $Al(NO_3)_3$ (Figure 9c). Furthermore, the accelerated dissolution rate of dolomite impurities (and other Ca/Mg-containing constituents) in the presence of H_2SO_4 has contributed to reduced Ca- and Mg-ion content within the structure of acid-activated bentonite specimens (Figures 9d and 9e). On the other hand, the augmented presence of Fe^{3+} and Mg^{2+} ions is due to the formation of Al-Mg-OH and intensified Al-Fe-OH bonds subsequent to Al^{3+} adsorption onto the bentonite surface, as also shown in FTIR results (see Figure 2). The high concentration of Fe^{3+} ions observed in the sample treated with 0.05 wt.% $Al(NO_3)_3$ appears inconsistent with other findings, likely attributed to experimental errors induced by impurities in the sample.

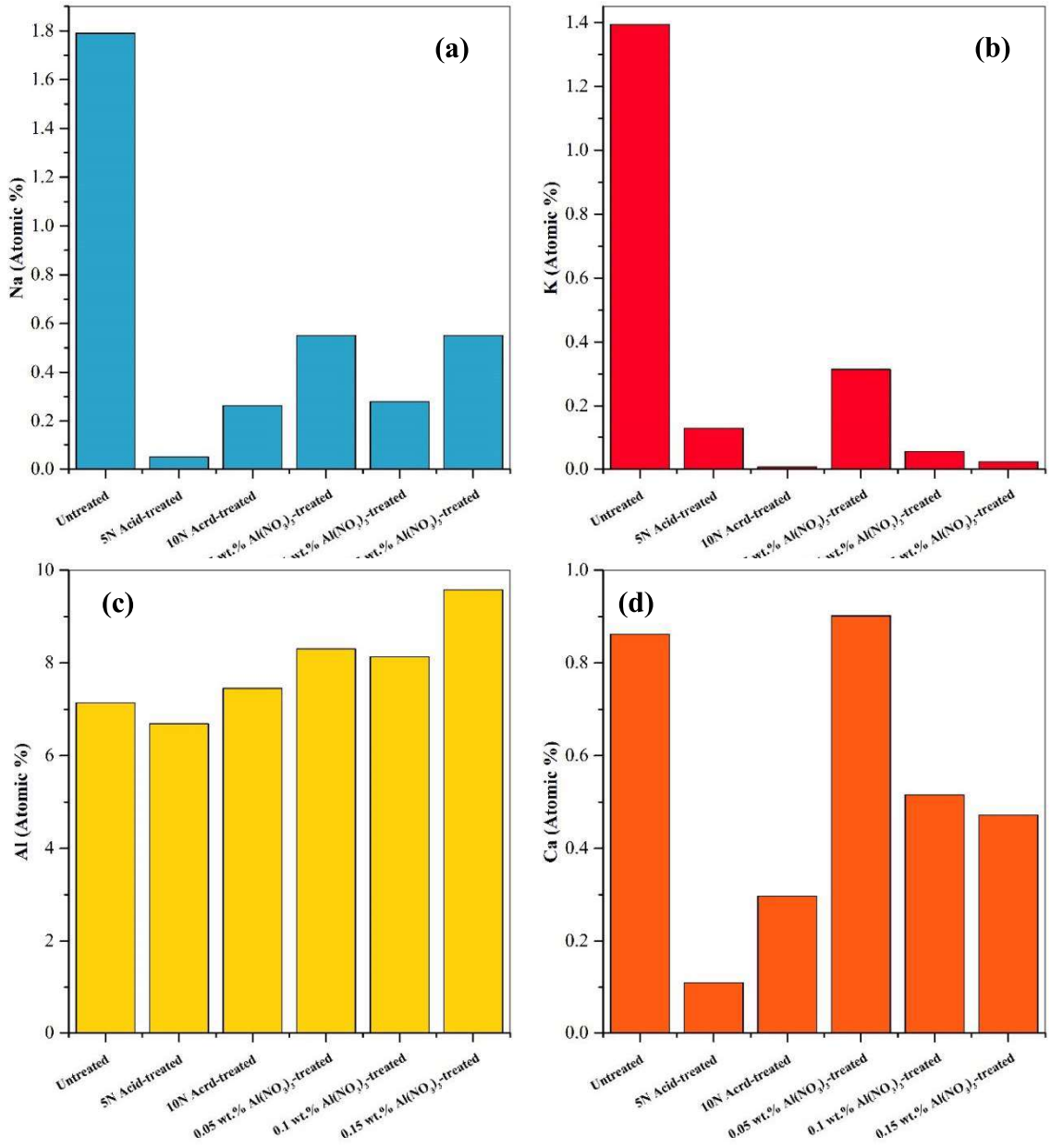
(a)
Na (Atomic %)
(b)
K (Atomic %)
(c)
Al (Atomic %)
(d)
Ca (Atomic %)
Untreated
5N Acid-treated
10N Acrd-treated
0.05 wt.% Al(NO3)3-treated
0.1 wt.% Al(NO3)3-treated
0.15 wt.% Al(NO3)3-treated

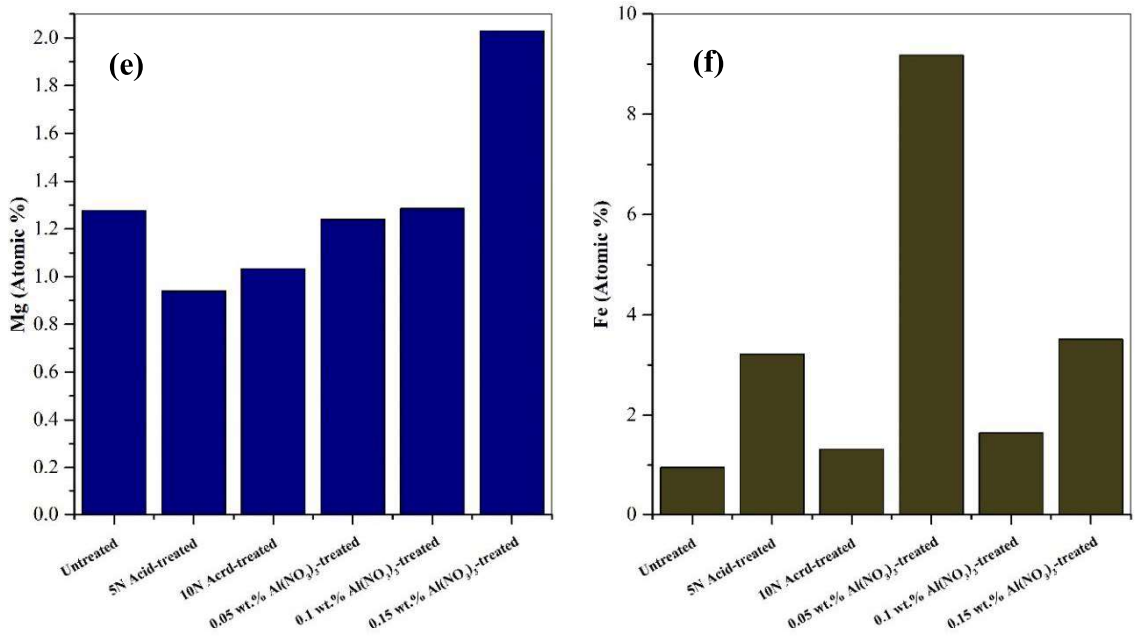

FIGURE 9: Cation contents of untreated and treated bentonites with varying acid and $Al(NO_3)_3$ concentrations (according to the results of EDS analysis).

Characterization of fluids prepared from surface-modified bentonites

Stability analysis

Figures 10 illustrates the results of stability analyses conducted on the aqueous solutions prepared from untreated and surface-treated specimens of bentonite, focusing on the free fluid (clear solution) level over a 60-minute duration at ambient temperature (see Figure 10a). In addition, a comparison between the 1-hr and 24-hr free fluid separation is presented in Figure 10b. As illustrated, the base fluid exhibits remarkable stability. The stability observed in untreated bentonite within the aqueous medium is attributed to its significant surface area, the high swelling capacity of bentonite in the presence of water, and the high electrostatic repulsion between negatively charged colloids[22, 48-51]. These features render gravitational forces ineffective in the exclusive removal of colloids during the sedimentation process.

Surface modification of bentonite using H_2SO_4 induces a decline in fluid stability, with a more pronounced reduction at higher acid concentration. The clear solution levels of these specimens exhibit a gradual reduction during the initial one-hour period (see Figure 10a). However, noteworthy is the substantial increase in final separation observed after a 24-hour testing duration (as illustrated in Figure 10b). The observed destabilization is ascribed to modified surface charge properties, reducing electrostatic repulsion between colloidal particles. As previously discussed, acid treatment induces cation exchange, substituting exchangeable cations on bentonite with protons, thereby altering its properties and destabilizing the fluid. The heightened acidity can even induce structural changes in bentonite, impacting its stability in the fluid. Acid modification also influences particle size distribution, affecting the fluid's rheological properties and stability[28, 31, 52]. Elevated H_2SO_4 concentration may potentially disintegrate the clay structure, causing increased aggregation and settling[52]. These cumulative

effects result in amplified bentonite hydrophobicity, promoted particle coagulation, diminished swelling capacity, thus, the reduced aqueous fluid stability.

The application of $Al(NO_3)_3$ similarly induced instability to the acid-treated method, especially evident at higher Al^{3+} concentrations (0.1 and 0.15 wt.%). The key distinction is the immediate impact on fluid stability, leading to the highest instability within the first hour, followed by a marginal increase in clear solution level throughout the rest of the experiment. In fact, the introduction of Al^{3+} reduces negative charges, enhancing hydrophobic forces and promoting colloidal agglomeration and settling[48, 49, 51]. The diminished settleability observed in bentonite clay suspensions at an Al^{3+} concentration of 0.05 ppm is associated with persistent negative charges on particles, indicating relative colloidal stability.

It is noteworthy that while visual observations imply clearer and faster colloidal separation in $Al(NO_3)_3$-treated bentonite (Figure 10), precise quantifications of free fluid levels (Figure 11) revealed a lower final height compared to acid-treated counterparts. This arises from the hydrophobic induction mechanism of $Al(NO_3)_3$, predominantly characterized by surface neutralization. In contrast, acid treatment employs surface protonation, inducing structural alterations, which results in a discernible reduction in Cation Exchange Capacity (CEC) within the bentonite samples, consequently decreasing their intrinsic swelling potential, leading to a lower height of free fluid separation.

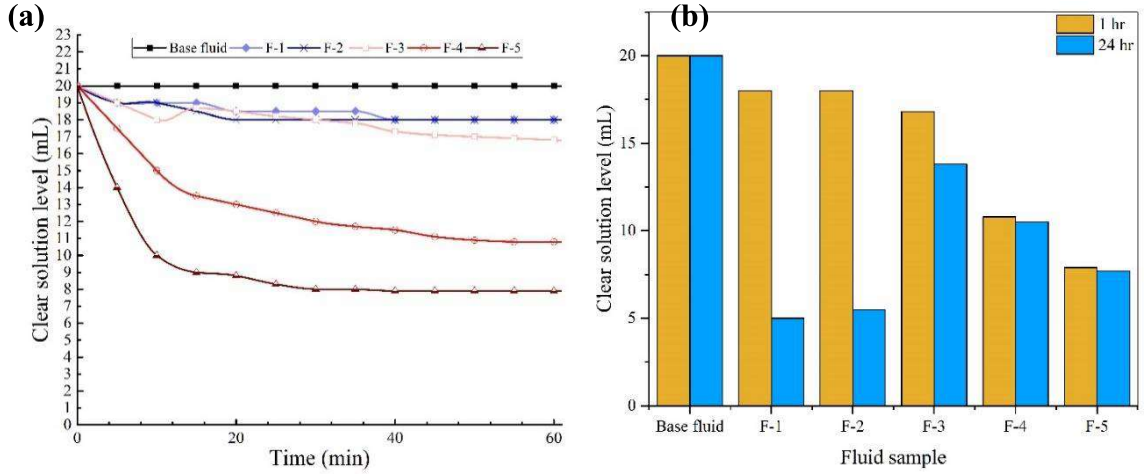

FIGURE 10: The results of stability analysis of base fluid (untreated), F-1 (5N acid-treated), F-2 (10N acid-treated), F-3 (0.05 wt.% $Al(NO_3)_3$-treated), F-4 (0.1 wt.% $Al(NO_3)_3$-treated), and F-5 (0.15 wt.% $Al(NO_3)_3$-treated).

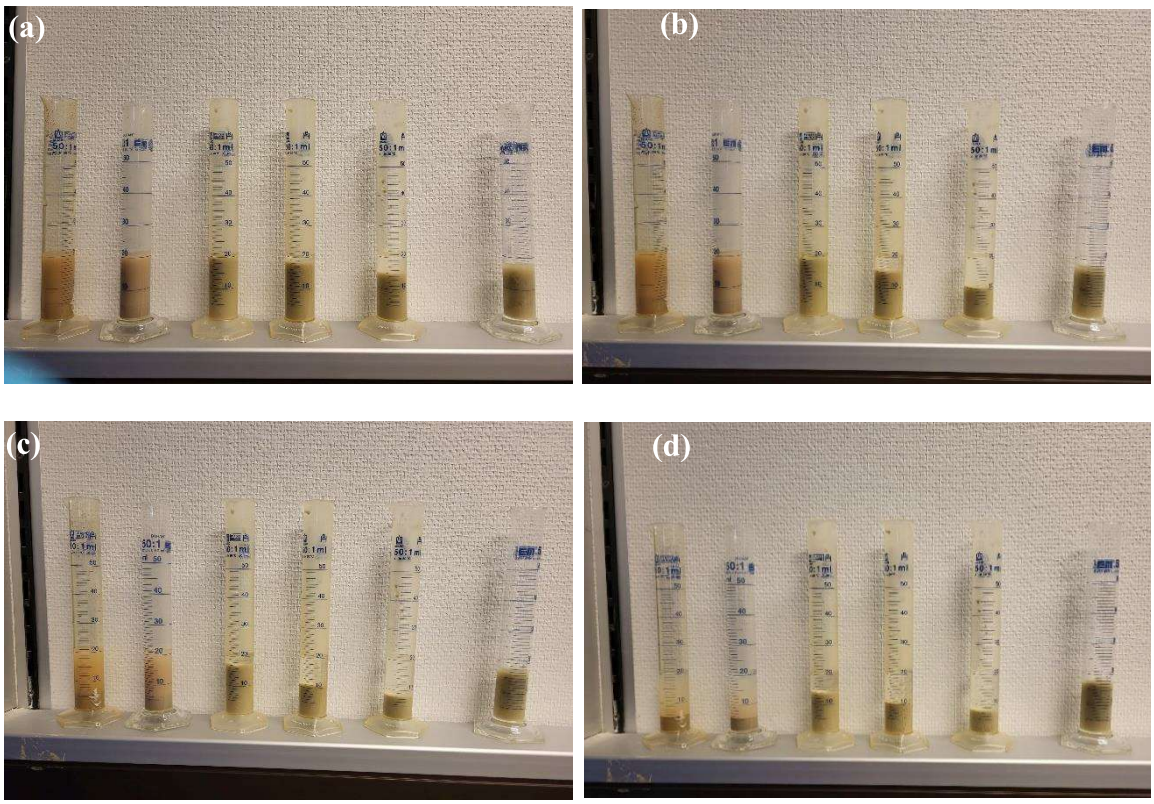

FIGURE 11: Stability analysis observations of fluids at (a) test initiation, (b) after 10 minutes, (c) after 1 hour, and (d) after 24 hours. In each image, the order from left to right includes F-1 (5N acid-treated), F-2 (10N acid-treated), F-3 (0.05 wt.% $Al(NO_3)_3$-treated), F-4 (0.1 wt.% $Al(NO_3)_3$-treated), F-5 (0.15 wt.% $Al(NO_3)_3$-treated), and base fluid (untreated).

Flow behavior analysis of modified fluids

As previously indicated, subsequent to the surface treatment of bentonite particles, a set of flow behavior analyses was conducted to assess the influence of surface modification approaches on the rheological characteristics of the resulting fluid. Figure 12 depicts the outcomes of flow behavior analysis conducted at ambient temperature, encompassing Base fluid, F-1 and F-2 (incorporating acid-treated bentonite), and F-3 to F-5 (incorporating $Al(NO_3)_3$-treated bentonite). The rheogram of the base fluid distinctly reveals a pronounced reduction in flow resistance concerning shear rate, indicative of the shear-thinning attributes inherent in bentonite-based fluids. This observed behavior predominantly arises from the degradation of the three-dimensional house-of-cards structure and the re-orientation of clay particles within the fluids in a position in favor of flow direction[18, 30, 53, 54].

The rheological behavior of the aqueous fluids formulated using the treated bentonite samples suggests the effective implementation of surface modification techniques, resulting in heightened hydrophobic characteristics of the bentonite surface and subsequent particle agglomeration. Consequently, the developed fluids demonstrate rheological properties closely resembling that of water, indicative of particle settlement due to the intensified hydrophobic forces. Note that, the surface treatment of bentonite using both modification approaches, irrespective of the acid normality and aluminium nitrate concentration, has resulted in lower shear stresses relative to shear rates when compared to the base fluid.

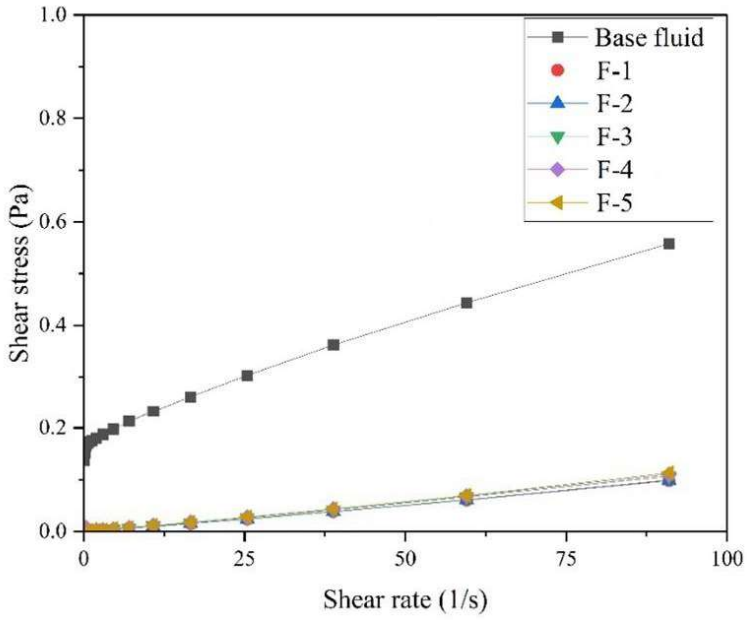

FIGURE 12: The results of rheological analysis of base fluid (untreated), F-1 (5N acid-treated), F-2 (10N acid-treated), F-3 (0.05 wt.% $Al(NO_3)_3$-treated), F-4 (0.1 wt.% $Al(NO_3)_3$-treated), and F-5 (0.15 wt.% $Al(NO_3)_3$-treated).

The results in Table 3 suggest a considerable decrease in the plastic viscosity (PV, μ_p) when the bentonite surfaces were treated with different acid normality and different $Al(NO_3)_3$ concentrations. When the bentonite surface was treated with $Al(NO_3)_3$, the PV decreased to 0.0012 Pa.s irrespective of concentration. Similar trends are observed in the yield point (YP, τ_0), with even 0.05 wt.% $Al(NO_3)_3$ causing substantial decreases in YP from 0.177 Pa (base fluid) to approximately 0.0006 Pa (F-3). Similarly, sharp decreases were observed in the PV and YP values when bentonite surfaces were treated with H_2SO_4. The diminished viscosifying capacity of the treated bentonites can be attributed to their reduced swelling degree in the presence of water, indicative of the less hydrophilic nature of the treated bentonite surface.

TABLE 3: Rheological analysis results from the Bingham models.

Parameter	Base Fluid	F-1	F-2	F-3	F-4	F-5
τ_0 (Pa)	0.177	0.0005	0.0007	0.0006	0.0009	0.0007
μ_p (Pa.s)	0.004	0.0011	0.0011	0.0012	0.0012	0.0012
R-Squared	0.9918	0.998	0.9985	0.9985	0.9912	0.998

SUMMARY AND CONCLUDING REMARKS

This research examined the characteristics of a bentonite sample prior to and subsequent to surface modification employing varying concentrations of $Al(NO_3)_3$, serving as a novel surface modification approach, and H_2SO_4, utilized as a control technique. The main objectives were to identify critical parameters influencing bentonite surface chemistry and to explore the potential of $Al(NO_3)_3$ in altering the properties of aluminosilicate samples towards a more hydrophobic nature. The study also evaluated Zeta-potential measurement, Fourier-transform infrared (FTIR) analysis, and scanning electron microscopy with energy dispersive spectroscopy (SEM-EDS) effectiveness in elucidating structural modifications induced by surface treatment approaches. Key findings are as follows:

Zeta Potential Analysis: The untreated bentonite exhibited a Zeta potential of -32.07 mV, signifying the presence of a stable colloidal solution. Subsequent treatment with 5N H_2SO_4 and 10N H_2SO_4 resulted in elevated Zeta potential values of -17.07 mV and -16.52 mV, respectively, indicating an augmented level of instability. The introduction of $Al(NO_3)_3$ to bentonite surface led to an increase in Zeta potential values, reaching the highest degree of instability (-14.62 mV) at 0.15 wt.% concentration. Despite adsorption and cation exchange processes, clay particles retained negative charges, mainly due to a higher prevalence of permanent surface charges on basal faces compared to edge charges, which are the primary candidates for cation exchange.

Micro-Scale Surface Characteristics: SEM and FTIR analyses of powdered bentonite samples following various treatments revealed notable changes in surface properties. Treatment with H_2SO_4 resulted in a constrained sheet-like structure and even disintegration of the clay at higher concentrations, linked to cation substitution and diminished electrostatic repulsion. This led to increased hydrophobicity, particle coagulation, and reduced swelling capacity of bentonite samples. Likewise, $Al(NO_3)_3$ treatment produced a compact smectite layer, with intensified agglomeration indicating elevated cation exchange. EDS analysis confirmed reduced monovalent ion concentrations, attributed to cationic exchange induced by H^+ and Al^{3+}. Moreover, EDS results demonstrated heightened adsorption of Fe^{3+} and Mg^{2+} ions on bentonite in the presence of Al^{3+}. This phenomenon, as indicated by FTIR results, is attributed to the formation of Al-Mg-OH and intensified Al-Fe-OH bonds following Al^{3+} adsorption onto the bentonite surface.

Stability and Rheological Behavior of the Resulting Fluids: The base fluid showed a high degree of stability arising from its substantial surface area, bentonite's high swelling capacity in water, and strong electrostatic repulsion between negatively charged colloids. H_2SO_4-induced surface modification decreased bentonite's stability, especially at higher acid concentrations, due to reduced electrostatic repulsion and increased hydrophobicity. The $Al(NO_3)_3$ treatment similarly induced instability, particularly at higher Al^{3+} concentrations, driven by increased metal hydroxide precipitates, accelerated aggregation, and heightened hydrophobicity. Reduced settleability at 0.05 wt.% $Al(NO_3)_3$ indicated relative colloidal stability, as confirmed by Zeta potential. Rheograms also showed shear-thinning behavior in all fluids, with treated bentonites exhibiting lower shear stresses, indicating less hydrophilic surfaces.

In summary, the obtained results highlighted the effectiveness of the suggested treatment technique, based on $Al(NO_3)_3$, for surface modification of bentonite clay, with practical

implications. While advancing the use of bentonite systems for challenging environments, variations influenced by the factors like ion type, and ion concentration suggest the need for further research to uncover specific mechanisms and unexplored aspects of treatment impacts on bentonite systems.

REFERENCES

(1) Israelachvili, J. N. *Intermolecular and surface forces*; Academic press, 2011.
(2) Van Oss, C.; Giese, R. Surface modification of clays and related materials. *Journal of dispersion science and technology* **2003**, *24* (3-4), 363-376.
(3) Giese, R. F.; Van Oss, C. J. *Colloid and surface properties of clays and related minerals*; CRC press, 2002.
(4) Keane, M. A. *Interfacial applications in environmental engineering*; CRC Press, 2002.
(5) Sulpizi, M.; Gaigeot, M.-P.; Sprik, M. The silica–water interface: how the silanols determine the surface acidity and modulate the water properties. *Journal of chemical theory and computation* **2012**, *8* (3), 1037-1047.
(6) Payne, C. C. Applications of colloidal silica: Past, present, and future. ACS Publications, 1994.
(7) Azam, S.; Darlington, A.; Gibbs-Davis, J. M. The influence of concentration on specific ion effects at the silica/water interface. *Journal of Physics: Condensed Matter* **2014**, *26* (24), 244107.
(8) Nayl, A.; Abd-Elhamid, A.; Aly, A. A.; Bräse, S. Recent progress in the applications of silica-based nanoparticles. *RSC advances* **2022**, *12* (22), 13706-13726.
(9) Huang, Y.; Li, P.; Zhao, R.; Zhao, L.; Liu, J.; Peng, S.; Fu, X.; Wang, X.; Luo, R.; Wang, R.; Zhang, Z. Silica nanoparticles: Biomedical applications and toxicity. *Biomedicine & Pharmacotherapy* **2022**, *151*, 113053. DOI: https://doi.org/10.1016/j.biopha.2022.113053.
(10) Kuciński, K.; Jankowska-Wajda, M.; Ratajczak, T.; Bałabańska-Trybuś, S.; Schulmann, A.; Maciejewski, H.; Chmielewski, M. K.; Hreczycho, G. Silica Surface Modification and Its Application in Permanent Link with Nucleic Acids. *ACS Omega* **2018**, *3* (6), 5931-5937. DOI: 10.1021/acsomega.8b00547.
(11) Hajiabadi, S. H.; Khalifeh, M.; van Noort, R.; Silva Santos Moreira, P. H. Review on Geopolymers as Wellbore Sealants: State of the Art Optimization for CO2 Exposure and Perspectives. *ACS Omega* **2023**.
(12) Hajiabadi, S.; Khalifeh, M.; Van Noort, R.; Moreira, P. S. S. Effect of magnesium-bearing additives on the properties of a granite-based geopolymer sealant for CCS. In *84th EAGE Annual Conference & Exhibition*, 2023; European Association of Geoscientists & Engineers: Vol. 2023, pp 1-5.
(13) Hajiabadi, S. H.; Khalifeh, M.; van Noort, R. Multiscale insights into mechanical performance of a granite-based geopolymer: Unveiling the micro to macro behavior. *Geoenergy Science and Engineering* **2023**, *231*, 212375. DOI: https://doi.org/10.1016/j.geoen.2023.212375.
(14) Xue, X.; Liu, Y.-L.; Dai, J.-G.; Poon, C.-S.; Zhang, W.-D.; Zhang, P. Inhibiting efflorescence formation on fly ash–based geopolymer via silane surface modification. *Cement and Concrete Composites* **2018**, *94*, 43-52.

(15) Lv, X.-s.; Qin, Y.; Lin, Z.-x.; Tian, Z.-k.; Cui, X.-m. Inhibition of Efflorescence in Na-Based Geopolymer Inorganic Coating. *ACS Omega* **2020**, *5* (24), 14822-14830. DOI: 10.1021/acsomega.0c01919.
(16) Pasupathy, K.; Ramakrishnan, S.; Sanjayan, J. Effect of hydrophobic surface-modified fine aggregates on efflorescence control in geopolymer. *Cement and Concrete Composites* **2022**, *126*, 104337. DOI: https://doi.org/10.1016/j.cemconcomp.2021.104337.
(17) Li, X.; Li, Z. Surface treatment of inorganic modifier for improving carbonation resistance of geopolymers. *Construction and Building Materials* **2023**, *400*, 132748. DOI: https://doi.org/10.1016/j.conbuildmat.2023.132748.
(18) Darzi, H. H.; Fouji, M.; Heidarabad, R. G.; Aghaei, H.; Hajiabadi, S. H.; Bedrikovetsky, P.; Mahani, H. Carbon-based nanocomposites: Distinguishing between deep-bed filtration and external filter cake by coupling core-scale mud-flow tests with computed tomography imaging. *Journal of Natural Gas Science and Engineering* **2022**, *105*, 104707.
(19) Binks, B. P.; Clint, J. H.; Whitby, C. P. Rheological behavior of water-in-oil emulsions stabilized by hydrophobic bentonite particles. *Langmuir* **2005**, *21* (12), 5307-5316.
(20) Zhang, R.; Zhu, X.; Cai, Y. The Phase Transformation Mechanism of Bentonite-Stabilized and Cetyltrimethylammonium Bromide-Stabilized Emulsions and Application in Reversible Emulsification Oil-Based Drilling Fluids. *Journal of Surfactants and Detergents* **2019**, *22* (3), 525-534.
(21) Mahmoud, A.; Gajbhiye, R.; Elkatatny, S. Application of organoclays in oil-based drilling fluids: a review. *ACS omega* **2023**, *8* (33), 29847-29858.
(22) Andrunik, M.; Bajda, T. Modification of bentonite with cationic and nonionic surfactants: Structural and textural features. *Materials* **2019**, *12* (22), 3772.
(23) Paria, S.; Khilar, K. C. A review on experimental studies of surfactant adsorption at the hydrophilic solid–water interface. *Advances in colloid and interface science* **2004**, *110* (3), 75-95.
(24) Ratkievicius, L. A.; Da Cunha Filho, F. J. V.; Neto, E. L. D. B.; Santanna, V. C. Modification of bentonite clay by a cationic surfactant to be used as a viscosity enhancer in vegetable-oil-based drilling fluid. *Applied Clay Science* **2017**, *135*, 307-312.
(25) Yang, C.; Zhu, Y.; Wang, J.; Li, Z.; Su, X.; Niu, C. Hydrothermal synthesis of TiO2–WO3–bentonite composites: conventional versus ultrasonic pretreatments and their adsorption of methylene blue. *Applied Clay Science* **2015**, *105*, 243-251.
(26) Booij, E.; Kloprogge, J. T.; Van Veen, J. R. Large pore REE/Al pillared bentonites: Preparation, structural aspects and catalytic properties. *Applied Clay Science* **1996**, *11* (2-4), 155-162.
(27) Shattar, S. F. A.; Zakaria, N. A.; Foo, K. Y. One step acid activation of bentonite derived adsorbent for the effective remediation of the new generation of industrial pesticides. *Scientific reports* **2020**, *10* (1), 20151.
(28) Carrado, K. A.; Komadel, P. Acid activation of bentonites and polymer-clay nanocomposites. *Elements* **2009**, *5* (2), 111-116.
(29) Hajiabadi, S. H.; Bedrikovetsky, P.; Mahani, H.; Khoshsima, A.; Aghaei, H.; Kalateh-Aghamohammadi, M.; Habibi, S. Effects of surface modified nanosilica on drilling fluid and formation damage. *Journal of Petroleum Science and Engineering* **2020**, *194*, 107559. DOI: https://doi.org/10.1016/j.petrol.2020.107559.
(30) Hajiabadi, S. H.; Aghaei, H.; Kalateh-Aghamohammadi, M.; Sanati, A.; Kazemi-Beydokhti, A.; Esmaeilzadeh, F. A comprehensive empirical, analytical and tomographic investigation on rheology and formation damage behavior of a novel nano-modified invert emulsion drilling fluid. *Journal of Petroleum Science and Engineering* **2019**, *181*, 106257.

(31) Tyagi, B.; Chudasama, C. D.; Jasra, R. V. Determination of structural modification in acid activated montmorillonite clay by FT-IR spectroscopy. *Spectrochimica Acta Part A: Molecular and Biomolecular Spectroscopy* **2006**, *64* (2), 273-278.
(32) D'Amico, D. A.; Ollier, R. P.; Alvarez, V. A.; Schroeder, W. F.; Cyras, V. P. Modification of bentonite by combination of reactions of acid-activation, silylation and ionic exchange. *Applied Clay Science* **2014**, *99*, 254-260. DOI: https://doi.org/10.1016/j.clay.2014.07.002.
(33) Maged, A.; Kharbish, S.; Ismael, I. S.; Bhatnagar, A. Characterization of activated bentonite clay mineral and the mechanisms underlying its sorption for ciprofloxacin from aqueous solution. *Environmental Science and Pollution Research* **2020**, *27*, 32980-32997.
(34) Widi, R. K.; Budhyantoro, A.; Christianto, A. Phenol hydroxylation on Al-Fe modified-bentonite: Effect of Fe loading, temperature and reaction time. In *IOP Conference Series: Materials Science and Engineering*, 2017; IOP Publishing: Vol. 273, p 012007.
(35) Chai, W.; Huang, Y.; Han, G.; Liu, J.; Yang, S.; Cao, Y. An enhanced study on adsorption of Al (iii) onto bentonite and kaolin: kinetics, isotherms, and mechanisms. *Mineral Processing and Extractive Metallurgy Review* **2017**, *38* (2), 106-115.
(36) Jardine, P.; Parker, J.; Zelazny, L. Kinetics and Mechanisms of Aluminum Adsorption on Kaolinite Using a Two-site Nonequilibrium Transport Model. *Soil Science Society of America Journal* **1985**, *49* (4), 867-873.
(37) Jardine, P.; Zelazny, L.; Parker, J. Mechanisms of aluminum adsorption on clay minerals and peat. *Soil Science Society of America Journal* **1985**, *49* (4), 862-867.
(38) Walker, W. J.; Cronan, C. S.; Patterson, H. H. A kinetic study of aluminum adsorption by aluminosilicate clay minerals. *Geochimica et Cosmochimica Acta* **1988**, *52* (1), 55-62.
(39) Tomić, Z. P.; Ašanin, D.; Antić-Mladenović, S.; Poharc-Logar, V.; Makreski, P. NIR and MIR spectroscopic characteristics of hydrophilic and hydrophobic bentonite treated with sulphuric acid. *Vibrational Spectroscopy* **2012**, *58*, 95-103.
(40) Kelessidis, V. C.; Tsamantaki, C.; Dalamarinis, P. Effect of pH and electrolyte on the rheology of aqueous Wyoming bentonite dispersions. *Applied Clay Science* **2007**, *38* (1-2), 86-96.
(41) Tombácz, E.; Szekeres, M. Surface charge heterogeneity of kaolinite in aqueous suspension in comparison with montmorillonite. *Applied Clay Science* **2006**, *34* (1-4), 105-124.
(42) Duc, M.; Gaboriaud, F.; Thomas, F. Sensitivity of the acid–base properties of clays to the methods of preparation and measurement: 1. Literature review. *Journal of colloid and interface science* **2005**, *289* (1), 139-147.
(43) Dodoo, D.; Fynn, G. E.; Yawson, E. S. C.; Appiah, G.; Suleiman, N.; Yaya, A. Eco-efficient treatment of hazardous bauxite liquid-residue using acid-activated clays. *Cleaner Chemical Engineering* **2022**, *3*, 100040. DOI: https://doi.org/10.1016/j.clce.2022.100040.
(44) Tabak, A.; Yilmaz, N.; Eren, E.; Caglar, B.; Afsin, B.; Sarihan, A. Structural analysis of naproxen-intercalated bentonite (Unye). *Chemical Engineering Journal* **2011**, *174* (1), 281-288.
(45) Goebbert, D. J.; Garand, E.; Wende, T.; Bergmann, R.; Meijer, G.; Asmis, K. R.; Neumark, D. M. Infrared spectroscopy of the microhydrated nitrate ions NO3−(H2O) 1− 6. *The journal of physical chemistry A* **2009**, *113* (26), 7584-7592.
(46) Ryan, P.; Huertas, F. J. The temporal evolution of pedogenic Fe–smectite to Fe–kaolin via interstratified kaolin–smectite in a moist tropical soil chronosequence. *Geoderma* **2009**, *151* (1-2), 1-15.
(47) Gonzalez-Estrella, J.; Ellison, J.; Stormont, J. C.; Shaikh, N.; Peterson, E. J.; Lichtner, P.; Cerrato, J. M. Saline brine reaction with fractured wellbore cement and changes in hardness and hydraulic properties. *Environmental Engineering Science* **2021**, *38* (3), 143-153.

(48) Baik, M. H.; Lee, S. Y. Colloidal stability of bentonite clay considering surface charge properties as a function of pH and ionic strength. *Journal of Industrial and Engineering Chemistry* **2010**, *16* (5), 837-841. DOI: https://doi.org/10.1016/j.jiec.2010.05.002.
(49) Yuan, G.; Cao, Y.; Schulz, H.-M.; Hao, F.; Gluyas, J.; Liu, K.; Yang, T.; Wang, Y.; Xi, K.; Li, F. A review of feldspar alteration and its geological significance in sedimentary basins: From shallow aquifers to deep hydrocarbon reservoirs. *Earth-science reviews* **2019**, *191*, 114-140.
(50) Yuan, H.; Deng, W.; Zhu, X.; Liu, G.; Craig, V. S. J. Colloidal systems in concentrated electrolyte solutions exhibit re-entrant long-range electrostatic interactions due to underscreening. *Langmuir* **2022**, *38* (19), 6164-6173.
(51) Paton, P.; Talens-Alesson, F. Effect of pH on the Flocculation of SDS Micelles by Al 3+. *Colloid and Polymer Science* **2001**, *279*, 196-199.
(52) Yildiz, N.; Aktas, Z.; Calimli, A. Sulphuric acid activation of a calcium bentonite. **2004**.
(53) Kazemi-Beydokhti, A.; Hajiabadi, S. H. Rheological investigation of smart polymer/carbon nanotube complex on properties of water-based drilling fluids. *Colloids and Surfaces A: Physicochemical and Engineering Aspects* **2018**, *556*, 23-29. DOI: https://doi.org/10.1016/j.colsurfa.2018.07.058.
(54) Luckham, P. F.; Rossi, S. The colloidal and rheological properties of bentonite suspensions. *Advances in Colloid and Interface Science* **1999**, *82* (1), 43-92. DOI: https://doi.org/10.1016/S0001-8686(99)00005-6.